Yung, K.L., Cheung, J.L.K., Chung, S.W. et al. A Single-Port Robotic Platform for Laparoscopic Surgery with a Large Central Channel for Additional Instrument. Ann Biomed Eng 45, 2211–2221 (2017).

Title: A Single-Port Robotic Platform for Laparoscopic Surgery with a Large Central Channel for Additional Instrument

Authors: Kai-Leung Yung[1], Sheung-Wai Chung[2] and Chung-Kwong Yeung[3]

Running head: Single-Port Robotic Platform with a Large Central Channel

Word count: 4575

Corresponding author:
Professor Chung-Kwong Yeung,
[3]NISI (HK) Limited
Tel: +852-2133-6083; Fax +852-2133-6000;
e-mail: ck.yeung@nisi.hk

Professor Kai-Leung Yung
[1]Department of Industrial and Systems Engineering,
The Hong Kong Polytechnic University;
email: kl.yung@polyu.edu.hk

Sheung-Wai Chung
[2]PolyU Technology & Consultancy Company Limited,
The Hong Kong Polytechnic University;
email: wils.chung@polyu.edu.hk

Abstract

We introduce an innovative surgical robotic platform for single incision laparoscopic or natural orifice transluminal endoscopic surgery which allows the insertion of up to four instruments including the robotic arms and the camera through a single cannula through the same footprint. After insertion of all instruments, a large central channel of Ø15mm diameter is kept clear for passage of additional laparoscopic instruments, such as the passage or retrieval of suture needles, and/or suction irrigators. This unique feature greatly facilitates the performance of complex surgical procedures. Phantom and animal trials have been performed to evaluate the insertion and retrieval sequences. Internally-motorized robotic arms with 7 degrees of freedom were used in both the phantom and animal trials. The whole platform, together with the 3 degrees of freedom swivel support that holds the cannula, has altogether 10 degrees of freedom to tackle complex surgeries and allows it to access all quadrants of abdominal cavity. This new single-port robotic platform paves a new development direction for future non-invasive surgery.

Key Terms—minimally invasive surgery, anchoring, laparoscopic surgery

I. INTRODUCTION

Minimally invasive surgery (MIS) has become an international standard over the past decade due to its proven advantages, such as small incisions, reduced blood loss, less postoperative pain, faster recuperation and shorter hospital stays compared to conventional open surgeries [16, 17, 21]. Robotic surgery represents the next frontier of MIS, greatly enhancing the surgeons' performance with substantial improvements in dexterity and ergonomics, as well as providing a remarkable magnified, 3-dimensional view of the surgical site [2, 15]. The da Vinci surgical system by Intuitive Surgical (CA, USA) which currently dominates the field of robotic surgery uses a multi-port approach, and as such requires multiple incisions for the insertion of various laparoscopic instruments into the abdominal cavity of the patient. The advantage of a multi-port system is that retrieval and re-insertion of the instruments during operation are quick and simple. In addition, the system uses externally actuated motors and thus size constraint of the robotic arms is not a problem as they do not occupy any space inside the abdomen. However, the disadvantages of this system, includes difficulties in patient repositioning, arm collisions, reversed hand-eye coordination and the ability to reach certain quadrants or parts of the abdominal cavity [19].

In order to reduce the invasiveness through decreasing the number of incisions, newer surgical paradigms including Single Port Laparoscopy (SPL)/LaparoEndoscopic Single-Site Surgery (LESS) and Natural Orifice Transluminal Endoscopic Surgery (NOTES), have been introduced leaving almost scarless results [1, 5, 6, 17]. Existing LESS and NOTES technologies necessitate the insertion of all laparoscopic instruments and camera through a single incision as most of these systems deploy an access port through a single incision where most commonly one vision unit and two manipulation arms are inserted for visualization and surgical interventions respectively[20]. The level of invasiveness would depend on the diameter of the access port which in turn affects the performance of the robotic arms. An access port with a smaller diameter can limit the dexterity of the distal effectors and the payload capacity due to the difficulty in miniaturizing electro-mechanical components while fulfilling the reduced invasiveness of the procedure. Degrees of freedom (DOF) of the robotic arms may also be compromised due to size constraints. The lack of optimal triangulation, reduced visual axis, field of view and significant impairment of surgeons' working ergonomics are also of considerations. Hence, it is always a challenge to minimize the system's access port size while maintaining the functionality and performance of the surgical robotic system[3, 10, 11].

To address the above insufficiencies, a novel single-port robotic system for laparoscopic surgery was developed. Current single port surgical systems require a large port size because instruments are inserted adjacent to each other. To reduce the port size and minimize the invasiveness to the patient, our robotic system allows sequential insertion of robotic arms, hence, the port size only needs to accommodate one instead of multiple adjacent instruments. Thus can offer tremendous flexibility to allow a surgeon to use other laparoscopic instruments and accessories without the need for additional ports. By virtue of its design, such a platform can readily be deployed for laparoscopic surgery through a natural orifice.

II. MATERIALS AND METHODS

A. The Robotic Platform

The robotic platform presented here comprise of an obturator, an inner tube, a cannula, end segments and spring plate assemblies attached to the proximal end of the robotic arms. Fig. 1(a) shows the components of the robotic platform. Briefly, the obturator is used to open the flaps attached to the distal ends of the cannula after the insertion of the instruments. The inner tube acts as the port to allow other instruments to pass through after the insertion of all the instruments as well as to support the deployed camera module arm and robotic arms. All the components, apart from entrance valve is made of stainless steel. The insertion of the cannula can allow a tilt angle of 70°on the patient's abdominal wall to allow a larger working envelope for the surgeon to reposition the robotic arms inside the abdominal cavity of the patient. Vision is provided by a 3D camera which is mounted at the distal end of the camera module arm. The robotic arms each have seven DOFs. The whole set-up is anchored to an external swivel system (not shown), which provides three additional DOFs, including longitudinal movement of the robotic arm (50mm), pitch (70°) and rotatory motion (180°).

B. Design

The anchoring and operating mechanism for this surgical robotic platform are governed by the design of the cannula, the spring lock, and lock pin and spring plate assembly attached to the end segment on the robotic arm. A more detailed analysis of each component is given in the following sub-sections.

B.1 Cannula

The cannula consists of an outer body, it serves as an access port and anchor point for the insertion of the camera module arm and the robotic arms. The outer and inner diameter of the cannula is 20mm and 16mm respectively. An inner tube is inserted into the cannula to support securely the arms and later to allow the insertion of additional instruments. The inner tube has an entrance valve made of polyurethane, that can substantially prevent gas exiting the access port and to maintain insufflation inside the abdominal cavity. Fig 1(b) shows the cannula with the entrance valve and the inner tube in position. The valve can be opened when additional laparoscopic instrument is inserted or retrieved through the cannula. Fig 1(c) shows cross-sectional

views of the insertion slots of the cannula. There are four insertion slots along the interior surface of the cannula outer body. The functions of these insertion slots are to guide and fix the spring plates and for cable management. Fig 1(d) shows a sectional view of the insertion slots of the cannula housing a cable and a spring plate. This is crucial for the insertion of subsequent instruments through the same space such that they would not interfere with the cables.

The cannula consists of four flaps that are attached to its distal end. The flaps functions as anchors when the camera module arm and robotic arms are inserted. The opening and closing mechanisms of the flaps are controlled by the hinges and the lock pins that are fixed to the interior of the cannula. Fig. 2(a) shows the position of the flaps in an open and close position. It also illustrates the positions of the hinges and lock pins that functions to secure the inserted arms in place after their insertion. The opening and closing of each flap is controlled by two hinges and one lock pin. Fig 2(b) shows a schematic diagram of the cannula with the inner tube in place supporting the robotic arms and the flaps in the open position.

B.2 Spring Lock

A spring lock is used to secure and lock the robotic arm to the flap of the cannula. The locking mechanism uses a dovetail joint. Primarily, the flaps on the cannula are kept closed with the lock pin in position. The spring lock on the flap is released by pushing on the lock pin (Fig 3(a)), when a robotic arm is inserted past the distal end of the cannula, the tail slot at the end segment will slide in the dovetail joint causing the spring lock to flip back to the locked position. Fig. 3(b) shows the end segment of the robotic arm with the flap and spring lock in place.

To determine if the weight of the robotic arm acting on the spring lock is sustainable, the shear stress was calculated using a worse-case gravitational pull as shown in Fig. 3(c). The parameters of the spring lock can be found in Table 1 and the calculation can be found in Table 2. The shear stress of the spring lock; $\tau_{spring\ lock}$ was determined to be 4.3MPa, which is below the shear stress at yield for stainless steel at 167 MPa.

B.3 Lock Pin

To deploy the robotic arm in position, an obturator is inserted into the cannula to push and swing the robotic arm outward to the working configuration position. The lock pin is then released to secure the robotic arm at this working position. This locking

feature ensures the robotic arm or any other instruments is securely anchored in place during their operation. The obturator can then be removed so the next instrument can be inserted through the cannula. Fig. 4 shows a schematic diagram of the lock pin position inside the cannula when the robotic arm is locked in its deployed position. The lock pin with diameter of d_p is used to provide pivoting of the robotic arm to a fixed position. The weight of the robotic arm W, at a lever length from the hinge to its center of mass (L_1) is supported by the lock pin which sustains a force at a lever length from the hinge (L_2). L_3 is the distance between the centre of the hinge and the proximal edge where the lock pin is anchored to, at the end segment of the robotic arm. In order to determine the total shear stress τ_{lp}, the magnitude of the force, f_p and axial load W_{rp}, was determined (Table 1 and 2). τ_{lp} was determined to be 112MPa, which is below the shear stress at yield (167 MPa) of the lock pin. Thus, validating that the lock pin in the cannula can sustain the weight of the robotic arm.

B.4 Spring Plate Assembly

The insertion and removal of the instruments in and out of the cannula is accomplished by using the spring plate assembly (Fig. 5(a)). This assembly consists of a spring plate and a handle which are laser-welded together, with one end of the spring plate attached to the end segment. The spring plate is curved in shape when in its normal form. The handle serves as an attachment for the ease of instrument retrieval. The spring plate also serves as a cable guard for cable management inside the cannula. When the spring plate assembly is fully inserted, the lower curved portion of the spring plate will straighten up and be locked in place by the lock pin. When instrument retrieval is desired, the lock pin will be released by pulling. The opposing force produced by the spring plate will produce a spring deflection helping the robotic arm to slightly swing away from the flap towards the centre of the cannula. Fig. 5(b) shows the deflection distance of the spring plate back to its normal form when the spring plate assembly is pulled out from the cannula. To determine the maximum allowable spring back force, maximum stress σ_{max} and maximum deflection y_{max} under uniform cross-section and uniform strength upon the spring plate was determined. Table 1 shows the parameters of the spring plate and methods of calculation is shown in Table 2. Results showed that the spring plate is able to provide a maximum allowable spring back force F, of 2.7N and a maximum deflection distance, y_{max}, of 2.6 mm.

C. Finite-element analysis

Finite-element analysis (SolidWorks, 2015) was used to simulate the cannula design and to determine if the lock pin can sustain the weight of the robotic arm. The simulation was performed without the inner tube and with the inner tube in place. Fig. 6 shows results of the stress analysis without the inner tube and indicate that stress sustainable was 19.6 MPa, which is below the yield stress of stainless steel (290 MPa). When the analysis was repeated with the inner tube inserted, and simulating a weight of 5N at the tip of the robotic arm, results showed that the maximum stress was 133.8 MPa, which is below the yield stress of the material used (290 MPa).

D. Insertion sequence

The insertion sequence for the robotic arms for this new robotic platform is illustrated in Fig. 7. Up to 4 robotic arms including a camera module can be inserted. The cannula is designed in such a way that the robotic arms are sequentially inserted parallel to the axis of the cannula. First, an abdominal incision is made and the cannula introduced through the abdominal wall using a sheath, (not shown). The insertion of the camera module is not included in this sequence. Fig 7(i) shows the insertion sequence of the first robotic arm into the cannula. The robotic arm is initially inserted until the end effector and the elbow joint passed the distal end of the cannula (Fig 7(ii)), where the forearm will be motor-driven to bend 90^{o} outwards (Fig 7(iii)), the insertion is further continued until the shoulder joint pass the cannula, where it will be motor-driven to bend 90^{o} outwards again to provide the working configuration of the robotic arms (Fig 7(iv)). To lock the arm to the cannula flap, an obturator is inserted which will then push against the end segment attached at the end of the robotic arm. The dovetail connection on the end segment will then lock the arm to the flap on the cannula. (Fig 7(v)). The insertion of the next arm will be done in similar manner to achieve the working configuration.

On complete insertion of standard instruments including a camera module and two standard robotic arms, a central lumen of the cannula is maintained with an inner diameter of Ø15mm, that can serve as an access port, free at all times, to accommodate the insertion of additional laparoscopic instruments, a feature that is not commonly found amongst other surgical systems.

III. EXPERIMENTS AND RESULTS

The components of the robotic platform were fabricated to validate the proposed design. Fig. 8(a) shows each fabricated component individually and after assembly showing the prototype of the robotic platform of the cannula with the spring lock, lock pins and spring plate assembly and the end segments of two robotic arms inside the cannula. A video is available to show the locking sequence. Fig. 8(b) shows the assembled robotic platform anchored onto a swivel, showing an additional standard laparoscopic instrument inserted through the central passage demonstrating that the central opening can accommodate additional instruments.

A series of experiments were carried out to evaluate the functionality of this platform. The cannula was tilted at various angles to mimic possible angles of trocar entry at surgery by measuring the force required to insert the robotic arm until the end segment was anchored to the flap of the cannula. Results (Table 3) show that, as the tilting angle increase, insertion force decrease and vice versa as the tilting angle increase, the force for retrieval force increase, demonstrating the ease of robotic arm insertion. The performance of the robotic platform was also evaluated by using master-slave control through a manipulator on the console. Dexterity and precision movements of the robotic arms were tested by knot tying. When a payload of 5N was applied to the robotic tip, with a distance of 0.166m from the distal end of the inner tube to the tip of the robotic arm, an equivalence of 0.83Nm torque was measured at the anchor point. No reactive movement was observed at the anchor, showing that the platform can securely support the robotic arms throughout the operation. This is consistent with the finite-element analysis.

The proposed platform was also evaluated by performing cholecystectomy in a non-survival porcine model Fig. 8(b). All the instruments were successfully inserted sequentially through the cannula. Electrical cables and spring plates were readily inserted along the insertion slots inside the cannula which thereafter enabled the insertion of other robotic arms with ease. It was also demonstrated that the spring lock was able to sustain the weight of the robotic arm, and to lock the robotic arm securely to the flap of the cannula. During the procedure, the gall bladder was lifted by the grasper and cauterization was performed. No undesirable reactive movement of the robotic arms was observed. Upon completion, all instruments were successfully retrieved using the spring plate assemblies.

IV. DISCUSSION

Constraints in single port robotic designs includes it size, force transmission and orientation to the workspace[4]. Two major configurations have been proposed to address these limitations; the type X and the type Y configurations. Typically type X single port robots face possible external arm collisions and inability to reach all quadrants of the abdomen without creating a new incision. In contrast, robots with the type Y configuration can prevent robotic arm collision and accessibility to an expanded workspace is possible through the same incision. The challenge of this type of robotic system is the way to provide adequate triangulation for the instruments[14]. Our robotic platform is built to address the limitations of existing robotics systems.

The diameter of the sheath used in a surgical robotic system is a key specification. A sheath with a larger diameter will be able to accommodate more dexterous and more powerful manipulative arms[20]. Most single port surgical robotic systems have their instruments inserted adjacent to each other[8, 9, 11, 12, 14, 19]. requiring a lumen size larger than the sum of the instruments diameters. As a result, the more instruments to be inserted, the larger the port size required, and thus a larger incision. A significant feature of our robotic platform which supersede other single port systems is the cannula design which uses flaps to swing out the camera module arm and robotic arms so they can be anchored to the side of the cannula retaining a clear passage for the insertion for other instruments through the same footprint. Not only a free passage is maintained at all times, but only a small incision to the patient's abdominal wall is required. A central channel with a maximum diameter of 15mm is left open for the insertion of other instruments such as surgical needle, hemostatic sponge or other assistive tools that are required by the surgeon. The changing of any inserted arms and instruments are made easy through the aid of the spring plate attached to the end segment. Any individual robotic arm can be retrieved by disengaging the lock pin and pulling on the spring plate to close the flap at the cannula. This design is crucial because the surgeon often requires to change instruments during operation e.g. from a cautery tool to a needle grasper. Not only does this expand the flexibility for surgeons the ease to use additional laparoscopic instruments for surgery, it also does not require a new incision to be made to the patient.

A number of research platforms based on single port access have been developed. These include the SPORT developed by Titan Medical Inc. which can be deployed through a 25mm incision with a payload of 3.25 N[13], SPRINT 2.0, constructed by Quaglia et al[12] that has a 34mm outer diameter and a payload of 5 N. Shin and Kwon

developed a robotic system that has a payload capable of more than 7.5 N with an 8mm manipulator[18]. Institutive Surgical Inc. introduced a recent development which uses a 25mm access port[7]. Our robotic platform can be introduced via an external sheath of diameter 25mm with a payload of 5 N. Many of the aforementioned robotic systems do not provide a central channel for insertion of extra instrument. *i-Snake* developed by Imperial College of London however do allow an additional channel for the insertion of a third instrument but the diameter of the channel is only 3mm. Due to its size, manipulation of larger organs was deemed challenging due to the amount of force which could be exerted by the instrument[14]. SPRINT 2.0 also allows a 8mm channel for insertion of an additional instruments. Our platform has a central channel of 15mm in diameter that can allow insertion of standard laparoscopic instruments through the inner tube. Such large channel is especially useful for the insertion of large size laparoscopic instrument e.g. stapler and specimen pouch like *Endo Catch*.

V. CONCLUSION

A single port robotic platform for LESS/NOTES has been introduced in this study. The main contribution of this design is the use of slots, flaps, lock pins and spring plates to resolve the issues associated with arbitrary insertion and retrieval of individual surgical robotic arms through the same space for single port robotic surgery system thus reducing the size of the incision. The system also resolves the problem of cables and other linkages for motion control of the robotic arms and their free retrieval in the middle of an operation. A large central channel of Φ15mm is also provided in this platform which enables the surgeon to insert additional instruments when necessary. The platform also allows the addition of a third robotic arm without increasing the port size further increasing the surgeon's flexibility, a much-needed feature that is not found in other surgical platforms. The platform is used with a 3 DOFs swivel device which can boast a 10 DOFs robotic system that can access all quadrants of the abdominal cavity. Phantom trial results on a functional prototype have validated the design objectives of this robotic platform. This new approach with fully internal-motorized robotic arms is paving the way for many complex NOTES procedures. Future works will further reduce the sizes of all the components and hence the overall size of the robotic platform.

ACKNOWLEDGMENT

This work is funded by the Innovation and Technology Commission of HKSAR (Project No.: ITS/149/13FX) and NISI (HK) Limited.

References

1. Asakuma, M., S. Perretta, P. Allemann, R. Cahill, S. A. Con, C. Solano, S. Pasupathy, D. Mutter, B. Dallemagne, and J. Marescaux. Challenges and lessons learned from NOTES cholecystectomy initial experience: a stepwise approach from the laboratory to clinical application. J. Hepatobiliary. Pancreat. Surg. 16:249-254, 2009.

2. Bhayani, S. B. and G. L. Andriole. Three-Dimensional (3D) Vision: Does It Improve Laparoscopic Skills? An Assessment of a 3D Head-Mounted Visualization System. Rev. Urol. 7:211-214, 2005.

3. Chandra, V., D. Nehra, R. Parent, R. Woo, R. Reyes, T. Hernandez-Boussard, and S. Dutta. A comparison of laparoscopic and robotic assisted suturing performance by experts and novices. Surgery 147:830-839, 2010.

4. Cheon, B., E. Gezgin, D. K. Ji, M. Tomikawa, M. Hashizume, H. J. Kim, and J. Hong. A single port laparoscopic surgery robot with high force transmission and a large workspace. Surg. Endosc. 28:2719-2729, 2014.

5. Ersin, S., O. Firat, and M. Sozbilen. Single-incision laparoscopic cholecystectomy: is it more than a challenge? Surg. Endosc. 24:68-71, 2010.

6. Kaouk, J. H., R. K. Goel, G. P. Haber, S. Crouzet, and R. J. Stein. Robotic single-port transumbilical surgery in humans: initial report. BJU Int. 103:366-369, 2009.

7. Kaouk, J. H., G. P. Haber, R. Autorino, S. Crouzet, A. Ouzzane, V. Flamand, and A. Villers. A novel robotic system for single-port urologic surgery: first clinical investigation. Eur. Urol. 66:1033-1043, 2014.

8. Lehman, A. C., J. Dumpert, N. A. Wood, L. Redden, A. Q. Visty, S. Farritor, B. Varnell, and D. Oleynikov. Natural orifice cholecystectomy using a miniature robot. Surg. Endosc. 23:260-266, 2009.

9. Leong, F., N. Garbin, C. D. Natali, A. Mohammadi, D. Thiruchelvam, D. Oetomo, and P. Valdastri. Magnetic Surgical Instruments for Robotic Abdominal Surgery. IEEE Rev. Biomed. Eng. 9:66-78, 2016.

10. Nicolau, S., L. Soler, D. Mutter, and J. Marescaux. Augmented reality in laparoscopic surgical oncology. Surg. Oncol. 20:189-201, 2011.

11. Payne, C. J., H. J. Marcus, and G. Yang. A Smart Haptic Hand- Held Device for Neurosurgical Microdissection. Ann. Biomed. Eng. 43:2185-2195, 2015.

12. Quaglia, C., G. Petroni, M. Niccolini, S. Caccavaro, P. Dario, and A. Menciassi. Design of a compact robotic manipulator for single- port laparoscopy.(Author abstract). Journal of Mechanical Design 136:105001, 2014.

13. Samson, H. Titan medical inc. completes functional prototype of its single port orifice robotic technology (SPORT(TM)) surgical system. Marketwired , 2013.

14. Shang, J., C. J. Payne, J. Clark, D. P. Noonan, K. W. Kwok, A. Darzi, and G. Z. Yang. Design of a Multitasking Robotic Platform with Flexible Arms and Articulated Head for Minimally Invasive Surgery. Rep. U. S. 2012:1988-1993, 2012.

15. Smith, R., A. Day, T. Rockall, K. Ballard, M. Bailey, and I. Jourdan. Advanced stereoscopic projection technology significantly improves novice performance of minimally invasive surgical skills. Surg. Endosc. 26:1522-1527, 2012.

16. Stiff, G., M. Rhodes, A. Kelly, K. Telford, C. P. Armstrong, and B. I. Rees. Long-term pain: less common after laparoscopic than open cholecystectomy. Br. J. Surg. 81:1368-1370, 1994.

17. Tacchino, R., F. Greco, and D. Matera. Single-incision laparoscopic cholecystectomy: surgery without a visible scar. Surg. Endosc. 23:896-899, 2009.

18. Won-Ho Shin and Dong-Soo Kwon. Surgical Robot System for Single- Port Surgery With Novel Joint Mechanism. Biomedical Engineering, IEEE Transactions on 60:937-944, 2013.

19. Wortman, T. D., K. W. Strabala, A. C. Lehman, S. M. Farritor, and D. Oleynikov. Laparoendoscopic single- site surgery using a multi- functional miniature in vivo robot. The international journal of medical robotics + computer assisted surgery : MRCAS 7:17, 2011.

20. Zhao, J., B. Feng, M. H. Zheng, and K. Xu. Surgical robots for SPL and NOTES: a review. Minim Invasive Ther. Allied Technol. 24:8-17, 2015.

21. Zornig, C., H. Mofid, A. Emmermann, M. Alm, H. A. von Waldenfels, and C. Felixmuller. Scarless cholecystectomy with combined transvaginal and transumbilical approach in a series of 20 patients. Surg. Endosc. 22:1427-1429, 2008.

Fig. 1(a) Major components in the single port robotic platform which includes the cannula, inner tube, insertion obturator, end segment and spring plate assembly attached to the end of the robotic arms.

Fig. 1(b) Position of the entrance valve for the insertion of additional instrument via the inner tube of the cannula.

Fig. 1(c) Viewing from the top of the cannula outer body, the positions of the four insertion slots and the access port.

Fig. 1(d) Top: Sectional view inside the cannula showing the empty slots for cable management. Bottom: insertion slots housing a cable and a spring plate.

Fig. 2(a) Cannula with the hinges and flaps shown in an open position and closed position

Fig. 2(b) Left: A schematic diagram of the cannula with the inner tube in place showing the open flaps with the end segment of robotics inserted. Right: A top view of the cannula with all four flaps in the opened position.

Fig. 3(a) Lock pin inside the cannula pushed in to unlock the spring lock insertion.

Fig. 3 (b) A lock pin which has been pulled back to allow the spring lock to automatically flip back to its locked position to lock the end segment of the robotic arm in place

Fig. 3 (c) A spring lock on the cannula showing a worse-case gravitational pull by the weight of a robotic arm.

Fig. 4 Schematic diagram of the lock pin position inside the cannula. The lock pin with diameter of d_p is used to provide pivoting of the robotic arm to a fixed position. The weight of the robotic arm W, at a lever length from the hinge to its center of mass (L_1) is supported by the lock pin which sustains a force at a lever length from the hinge (L_2). L_3 is the distance between the centre of the hinge and the proximal edge where the lock pin is anchored to, at the end segment of the robotic arm.

Fig. 5(a) A spring plate assembly attached to the end segment of a robotic arm

Fig. 5(b) Deflection distance of the spring plate when it is pulled at the handle for its retrieval

Fig. 6 Results of the Finite-element analysis. Left: Finite-element analysis on the stress sustained of the designed platform on the weight of the robotic arm before insertion of the inner tube. Right: Finite-element analysis on the stress sustained of the designed platform with the inner tube inserted and a 5N weight at the tip of the robotic arm.

Fig. 7(a) Insertion sequence of the robotic platform. The insertion of the camera module is not included in this sequence. (i) shows the insertion of the first robotic arm into the cannula. (ii) the robotic arm inserted until the end effector and the elbow joint passed the distal end of the cannula. (iii) forearm will be motor-driven to bend 90^{o} outwards. (iv) the robotic arm is inserted further until the shoulder joint pass the cannula, where it will be motor-driven to bend 90^{o} outwards. (v) the arm is push outwards and locked to the cannula flap by the dovetail connection on the end segment of the robotic arm.

Fig. 8(a) Left: Fabricated components of the robotic platform shown individually. Right: the assembled prototype of the cannula with the spring lock and end segments of the robotic arms.

Fig. 8(b) Left: The robotic platform showing the central channel with an additional standard laparoscopic instrument passing through. Right: The robotic platform with the camera arm module and robotic arms in porcine trial.

Fig 1(a)

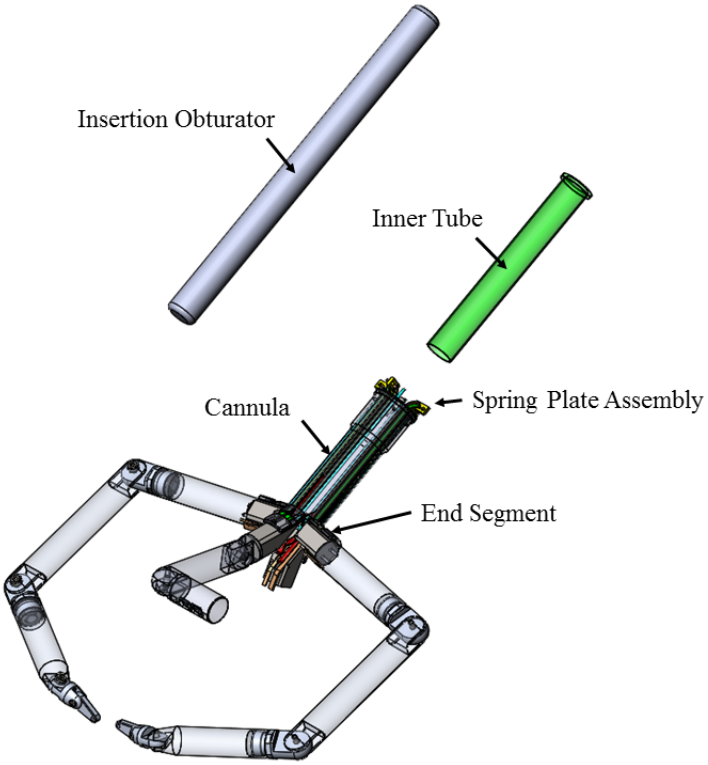
Insertion Obturator
Inner Tube
Cannula
Spring Plate Assembly
End Segment

Fig 1(b)

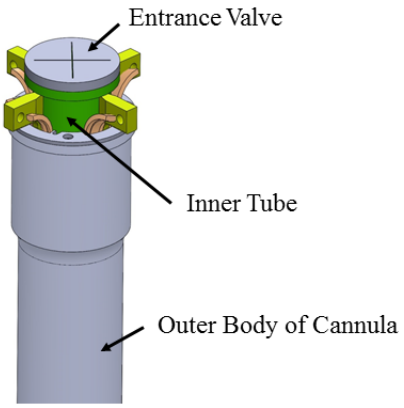
Entrance Valve
Inner Tube
Outer Body of Cannula

Fig 1(c)

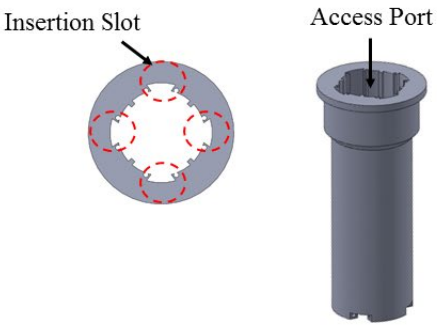

Fig 1(d)

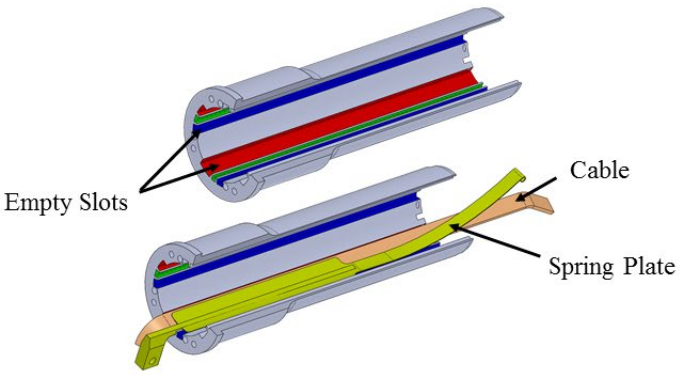

Fig 2(a)

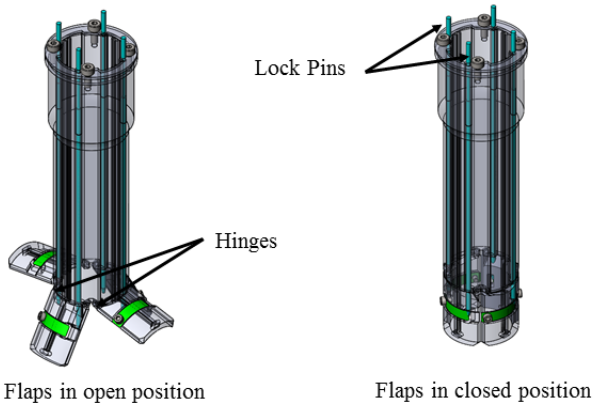
Lock Pins
Hinges
Flaps in open position
Flaps in closed position

Fig 2(b)

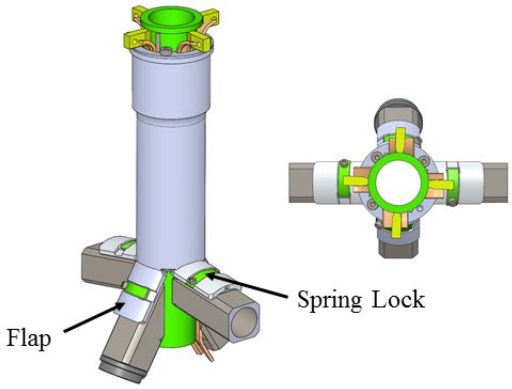
Spring Lock
Flap

Fig 3(a)

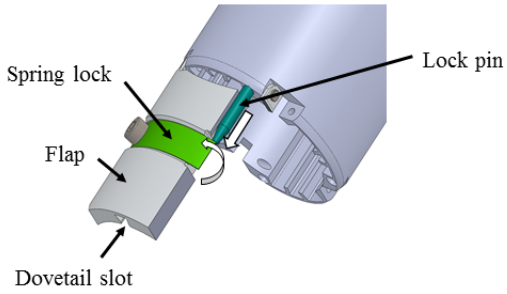
Spring lock
Lock pin
Flap
Dovetail slot

Fig 3(b)

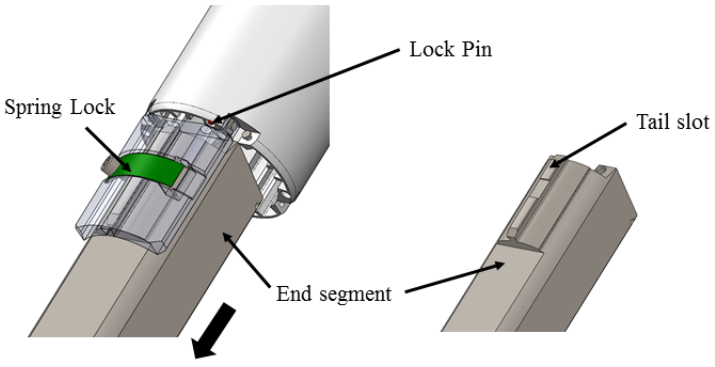
Lock Pin
Spring Lock
Tail slot
End segment

Fig 3(c)

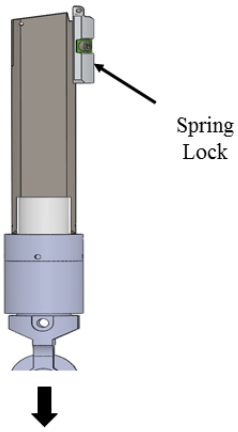

Fig 4

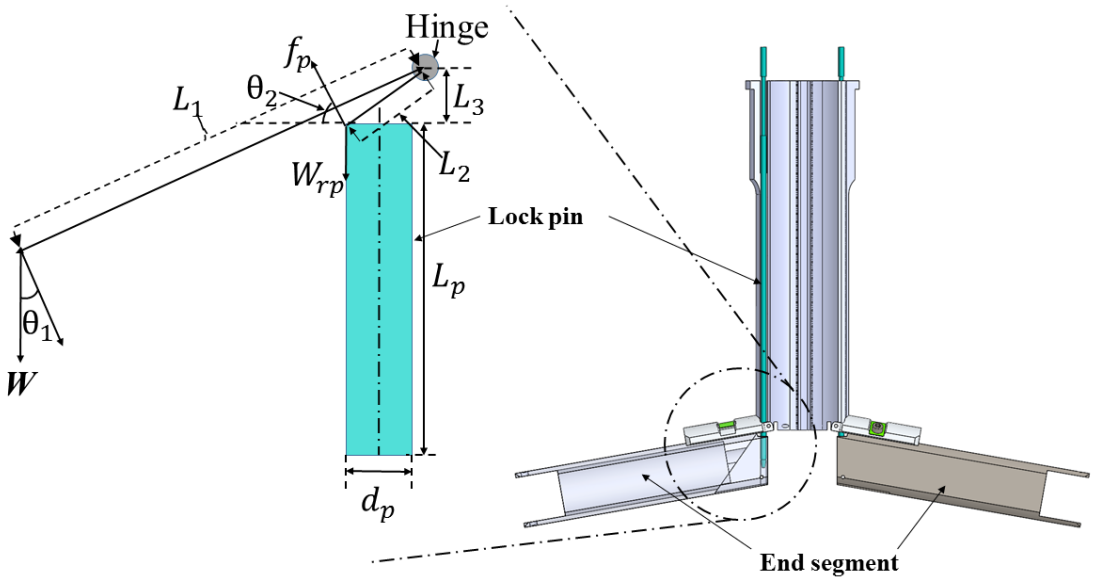
Hinge
f_p
θ_2
L_1
L_3
L_2
W_{rp}
Lock pin
L_p
θ_1
W
d_p
End segment

Fig 5(a)

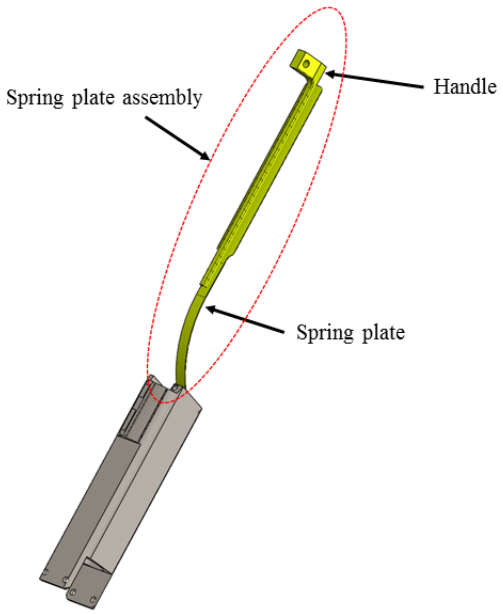
Spring plate assembly
Handle
Spring plate

Fig 5(b)

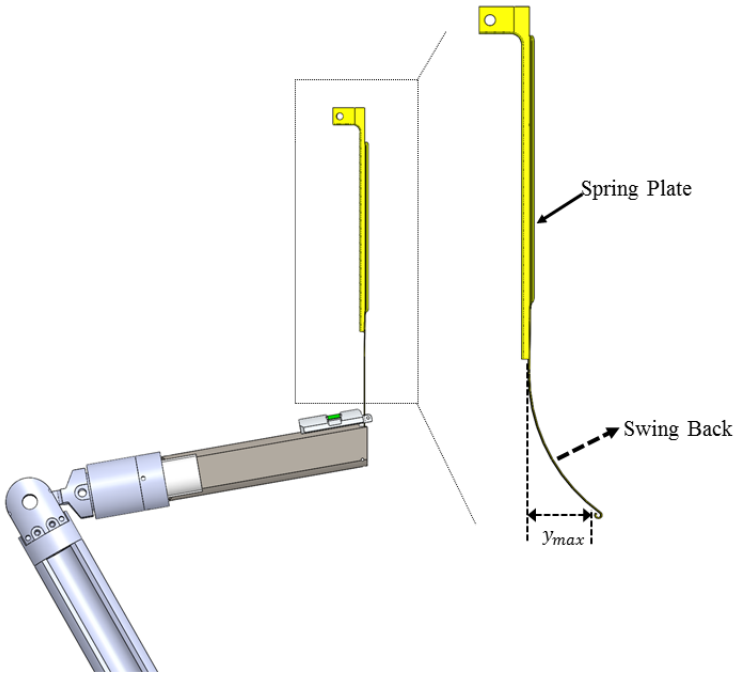
Spring Plate
Swing Back
y_{max}

Fig 6

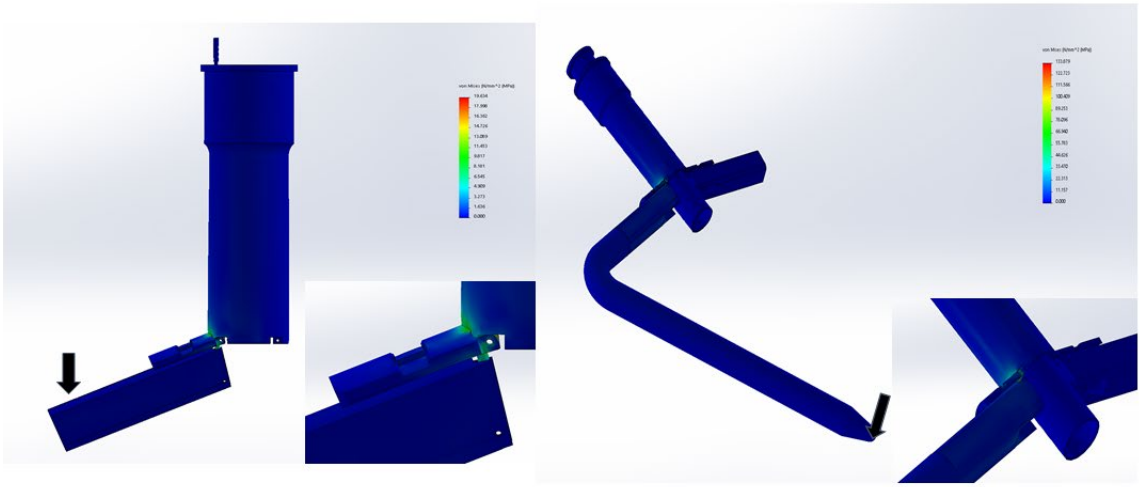

Fig 7

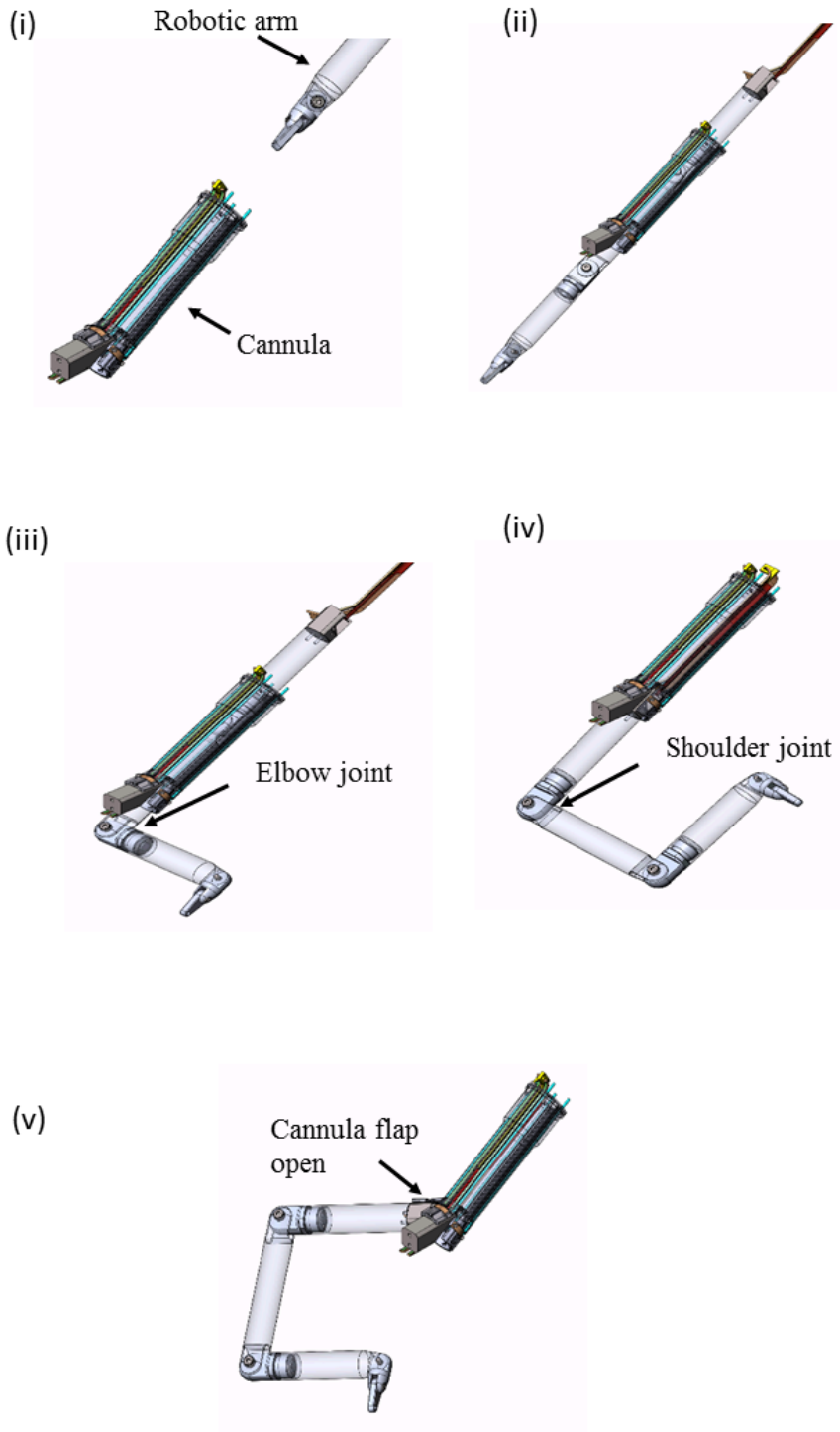
(i)
Robotic arm
Cannula
(ii)
(iii)
Elbow joint
(iv)
Shoulder joint
(v)
Cannula flap
open

Fig 8(a)

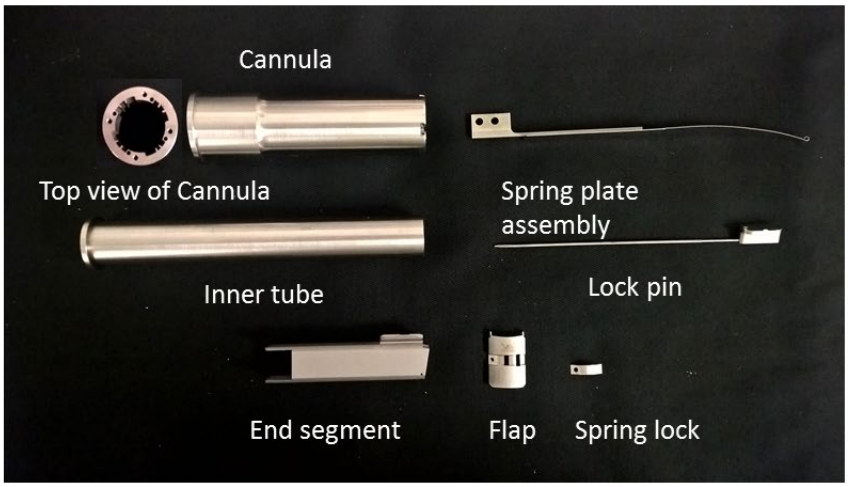
Cannula
Top view of Cannula
Spring plate assembly
Inner tube
Lock pin
End segment
Flap
Spring lock

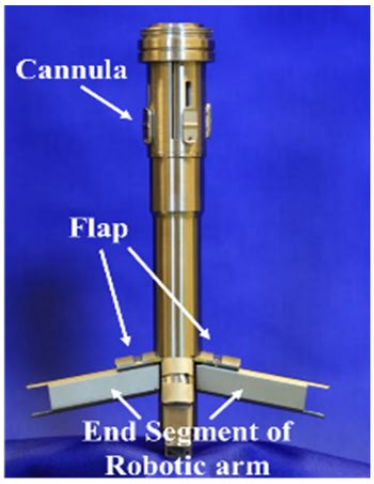
Cannula
Flap
End Segment of Robotic arm

Fig 8(b)

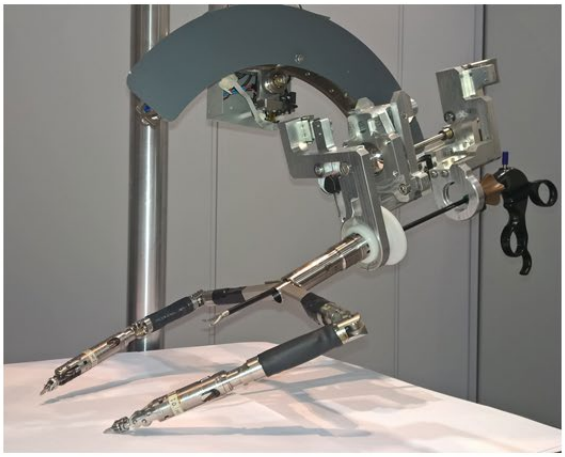

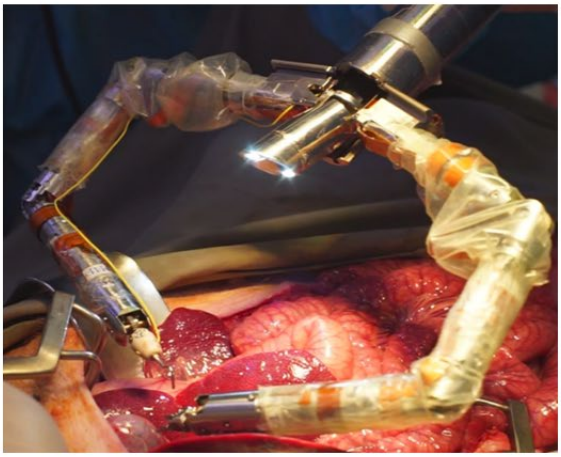

Table 1. Parameters of the components

Parameter	Measurement (unit)	
Robotic arm		
Weight (W)	2.25	N
Spring Lock		
Length (l)	3.5	mm
Thickness (t)	0.15	mm
Cross-section area	0.53	mm^2
Lock Pin		
L_1	58.2	mm
θ_1	55	degrees
L_2	7.6	mm
L_3	3.2	mm
θ_2	15	degrees
d_p	1.4	mm
Spring Plate		
Length (l)	27	mm
Width (w)	3.5	mm
Thickness (t)	0.5	mm
Modules of elasticity (E)	190	GPa

Table 2. Methods of calculations

Parameter	Calculations
Spring Lock	
$\tau_{spring\ lock} = \frac{W}{cross-section\ area\ of\ spring\ lcok}$	$\tau_{spring\ lock}$= 4.3 MPa
Lock Pin	
$W\cos\theta_1 L_1 = f_p L_2$	f_p = 23.5 N
$\tau_{lp} = \frac{32 f_p L_3 \cos\theta_2}{\pi {d_p}^3} + \frac{4 f_p \sin\theta_2}{\pi {d_p}^2}$	τ_{lp}= 112 MPa
Spring Plate	
$F = \frac{\sigma_{max} b t^2}{6l}$	F= 2.7 N
$y_{max} = \frac{4Fl^3}{bt^3E}$	y_{max}=2.6 mm

Table 3. Insertion and retrieval force of the robotic arm to the cannula

	Force (N)			
Insertion angle (Degrees)	**Trial 1**	**Trial 2**	**Trial 3**	**Mean**
0	7.3	7.5	7.6	7.5
7.5	6.4	6.4	6.8	6.5
15	5.5	5.5	5.7	5.6
Retrieval angle (Degrees)	**Trial 1**	**Trial 2**	**Trial 3**	**Mean**
0	7.1	7.7	7.1	7.3
7.5	9.5	10.4	10.3	10.1
15	11.5	11.6	11.2	11.4